Advances in
Science & Research
Open Access Proceedings

Large-Eddy Simulation of plume dispersion within various actual urban areas

H. Nakayama[1]**, K. Jurcakova**[2]**, and H. Nagai**[1]

[1]Japan Atomic Energy Agency, Ibaraki, Japan
[2]Institute of Thermomechanics, Academy of Sciences of the Czech Republic, Prague, Czech Republic

Correspondence to: H. Nakayama (nakayama.hiromasa@jaea.go.jp)

Abstract. Plume dispersion of hazardous materials within urban area resulting from accidental or intentional releases is of great concern to public health. Many researchers have developed local-scale atmospheric dispersion models using building-resolving computational fluid dynamics. However, an important issue is encountered when determining a reasonable domain size of the computational model in order to capture concentration distribution patterns influenced by urban surface geometries. In this study, we carried out Large-Eddy Simulations (LES) of plume dispersion within various urban areas with a wide range of obstacle density and building height variability. The difference of centerline mean and r.m.s. concentration distributions among various complex urban surface geometries becomes small for downwind distances from the point source greater than 1.0 km. From these results, it can be concluded that a length of a computational model should be at least 1.0 km from a point source.

1 Introduction

Plume dispersion within urban area resulting from accidental or intentional releases of hazardous materials is of great concern to public health. For the assessment of human health hazards or the safety analysis of flammable gases from such hazardous substances, the existence of instantaneous high concentrations in a plume should be considered. In such a situation, it is necessary to accurately predict not only the average levels but also the instantaneous magnitudes of concentration of a plume, considering the effects of individual urban buildings and obstacles.

For investigating behaviours of a plume in urban areas, a numerical modelling is a useful tool. Many researchers have developed local-scale atmospheric dispersion models using computational fluid dynamics (CFD). For example, Boris (2002) has developed a building-resolving CFD model (FAST3D-CT) that can simulate realistic features of urban flow and plume dispersion. Baklanov and Nuterman (2009) have developed a micro-scale model for urban environment (M2UE). This is a comprehensive CFD-type building-resolving urban wind and dispersion model. Armand et al. (2011) has designed an atmospheric transport model called as Micro-SWIFT-SPRAY (MSS). The special features of this model are to simulate plume dispersion in urban areas by a mass consistent wind field approach in a reduced computing time compared with CFD-based dispersion models. These models can provide detailed information on turbulent flows and plume concentrations in urban areas where individual buildings are explicitly resolved. However, an important issue is encountered when determing a reasonable domain size of the computational model in order to capture the distribution patterns of plume concentrations influenced by urban surface geometries. Actual urban surface geometries are very complex because the grounds are highly inhomogeneous and covered with low- and high-rise buildings with very variable heights. Lower part of atmospheric boundary layer called as roughness sub-layer is strongly influenced by the individual roughness obstacles that bring about strong three-dimensionality of the flow. Therefore, the shape and extent of the plume also become highly complex within urban canopy.

In this study, we carry out CFD simulations of plume dispersion within various urban areas with a wide range of
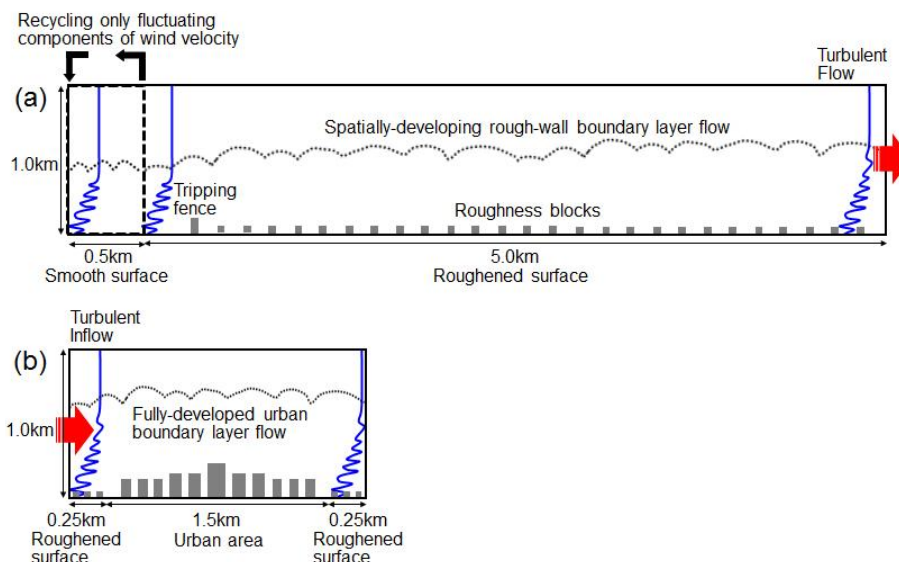
Figure 1. Schematic diagram of numerical model. **(a)** Driver region for generating a rough-wall turbulent boundary layer flow. **(b)** Main analysis region for plume dispersion in various urban areas.

obstacle density and building height variability, and clarify the spatial extent of concentration distribution patterns influenced by the urban surface geomeries by comparative analysis.

2 Computational model and settings

2.1 Numerical model

The CFD technique has been recognized as a helpful tool with the rapid development of computational technology. In particular, there are two different approaches to simulate turbulent flows: the Reynolds-Averaged Navier-Stokes (RANS) and Large-Eddy Simulation (LES) models. Tominaga and Stathopoulos (2010, 2011) investigated the difference of the basic performance between RANS and LES in modeling dispersion fields in an isolated building and in a street-canyon. They showed that the lateral dispersion behaviors of a plume are reproduced by LES better than RANS. Therefore, LES is applied in this study because we focus on the lateral extent of plume concentrations influenced by urban surface geometries characterized by individual buildings or street-canyons.

The basic equations of our LES model (Nakayama et al., 2013) are the filtered continuity equation, the Navier-Stokes equation, and the scalar conservation equation. The subgrid-scale turbulent effect is represented by the standard Smagorinsky model (1963) with the constant value of 0.1. The subgrid-scale scalar flux is also parameterized by an eddy viscosity model. The turbulent Schmidt number is set to 0.5. The building effect is represented by immersed boundary method proposed by Goldstein et al. (1993). This external force term is introduced into the Navier-Stokes equation.

The coupling algorithm of the velocity and pressure fields is based on the marker-and-cell method (Harlow and Welch, 1965) with the second-order Adams-Bashforth scheme for time integration. The Poisson equation is solved by the successive over-relaxation method. For the spatial discretization in the basic equations, a second-order accurate central difference scheme is used. However, for the advection term of the scalar conservation equation, cubic interpolated pseudo-particle (Takewaki et al., 1985) is used.

2.2 Computational model and boundary conditions

Figure 1 shows a schematic diagram of the computational model. Two computational domains are set up. One is a driver region for generating a rough-wall boundary layer flow and the other is a main analysis region for LESs of plume dispersion in urban areas. In the driver region, first, a basic turbulent boundary layer flow is generated at the upstream part by the recycling technique of Kataoka and Mizuno (2002) and then a wind flow with strong turbulent fluctuations is produced by a tripping fence and roughness blocks placed at the downstream of the recycle station. This turbulent inflow data is imposed at the inlet of the main region at each time step and LESs of urban plume dispersion are carried out.

Assuming that the scale of the simulated boundary layer by the LES is 400 m in the full scale condition, the size of the driver region is $5.5\,km \times 1.0\,km \times 1.0\,km$ in streamwise, spanwise and vertical directions, respectively. The number of grid points is $460 \times 250 \times 90$. The streamwise and vertical grid spacing is stretched from 4.0 to 20 m and from 1.3 to 53 m, respectively. The spanwise grid spacing is 4.0 m. The number of grid points and the size for a tripping fence and each roughness block are $7 \times 250 \times 24$ and $3 \times 6 \times 12$ grids, and
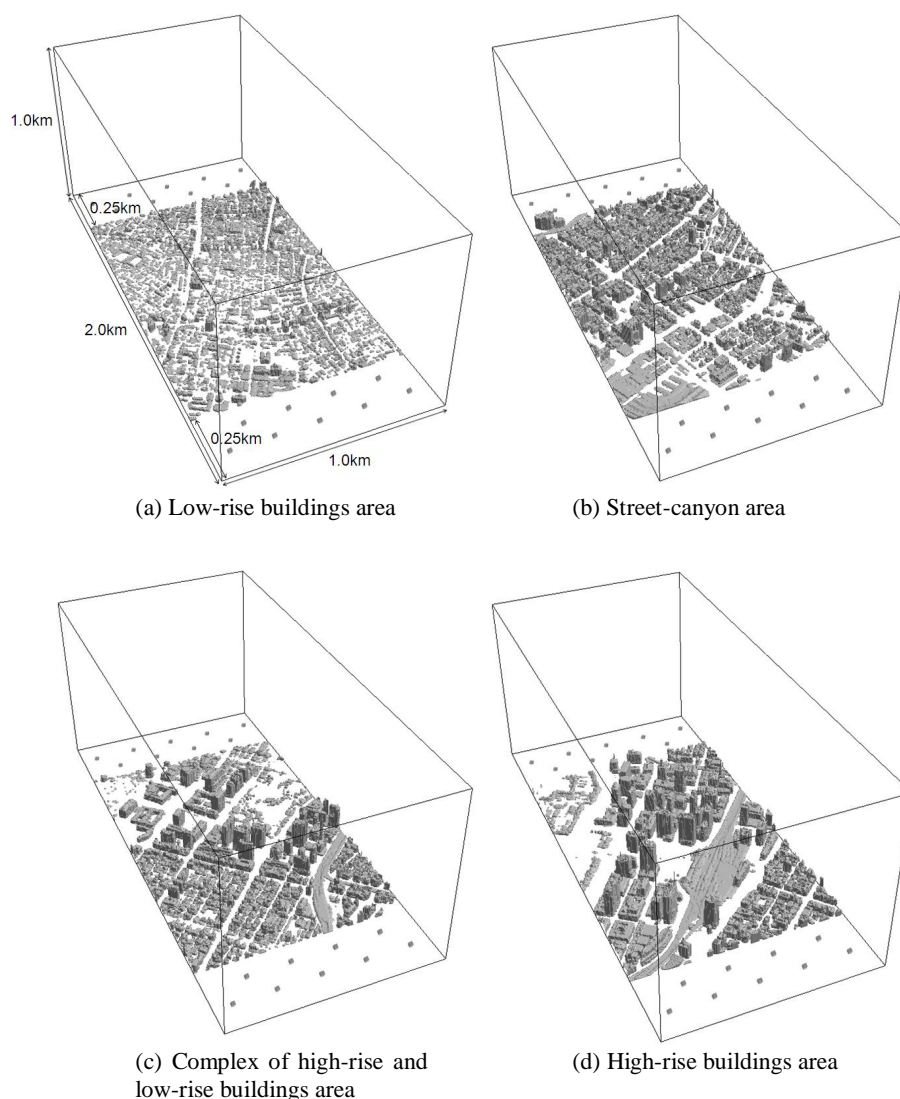
(a) Low-rise buildings area

(b) Street-canyon area

(c) Complex of high-rise and low-rise buildings area

(d) High-rise buildings area

Figure 2. Computational models for LES calculation cases.

$25.2\,\text{m} \times 1000\,\text{m} \times 26.4\,\text{m}$ and $10.8\,\text{m} \times 10.8\,\text{m} \times 9.6\,\text{m}$ in the streamwise, spanwise and vertical directions, respectively. In the main region, the size and the number of grid points are $2.0\,\text{km} \times 1.0\,\text{km} \times 1.0\,\text{km}$ and $375 \times 250 \times 90$ grids in streamwise, spanwise and vertical directions, respectively as shown in Fig. 2. The size of the domain where an urban surface geometry is resolved is $1.5\,\text{km}$ (streamwise) $\times 1.0\,\text{km}$ (spanwise) with the depth of $1.0\,\text{km}$. Roughened surfaces are set up with a $250\,\text{m}$ length at the up- and downstream of the urban area. The lateral grid spacing is $4.0\,\text{m}$. The vertical grid spacing is the same as the one in the driver region.

Franke et al. (2007) and Tominaga et al. (2008) proposed the guidelines for CFD simulations of wind environment in urban areas and showed the appropriate computational domain size, representation of surroundings, grid discretization, and boundary conditions. Our model is basically designed

based on the guidelines except a grid arrangement. Almost buildings and street canyons are resolved by 10 grid points at most in the lateral direction. According to the guideline, the minimum grid resolution should be 10 grid points to reproduce separating flows around buildings. However, our focus is on the general distribution patterns of plume concentrations depending on urban surface geometries. We consider that the differences of plume concentrations among various urban areas can be quantitatively captured by this LES model.

At the exit of the driver and main regions, the Sommerfeld radiation condition (Gresho, 1992) is applied. At the top, a free-slip condition is imposed for streamwise and spanwise velocity components and vertical velocity component is 0. At the side, a periodic condition is imposed. At the ground surface, a non-slip condition is imposed for each

Table 1. Cases for comparative analysis.

Surface geometry type		Average building height [m]	Building height variability [–]	Obstacle density [–]
Idealized urban canopy (Bezpalcova and Ohba, 2008 and LESs)	Cubic buildings array	28.0	0.0	0.16
	Cubic buildings array	28.0	0.0	0.25
	Cubic buildings array	28.0	0.0	0.33
Actual urban site in Central Tokyo (present LESs)	Low-rise buildings area	9.6	0.60	0.39
	Street-canyon area	22.7	0.71	0.56
	Complex of high-rise and low-rise buildings area	26.5	0.85	0.52
	High-rise buildings area	34.1	0.94	0.52

velocity component. The time step interval $\Delta t U_\infty / H$ is about 0.0005. Here, Δt, U_∞, and H indicate time step, a free-stream velocity, and a height of the computational domain, respectively. The maximum Courant-Friedrich-Levy number is about 0.15. The length of the simulation run to calculate the time averaged values $T U_\infty / H$ (T: averaging time) is set at 500 to obtain a steady-state concentration field. The length of the simulation run before releasing the scalar is $T U_\infty / H$ is 250.

2.3 Cases for comparative analysis

Table 1 lists cases for comparative analysis. We deal with two types of urban surface geometries. One is idealized urban canopy represented by regularly square array of cubic buildings with average building height of 28 m and obstacle density of 0.16, 0.25, and 0.33, respectively. Here, obstacle density and building height variability are defined as the ratio of the total frontal area of buildings to the study site and the ratio of the standard deviation of building height to the average building height of the study site. These cases were examined by wind tunnel experiments of Bezpalcova and Ohba (2008) and LESs (Nakayama et al., 2013). In their experiments, there are 15×7, 18×9, and 20×9 building arrays with $\lambda_f = 0.16$, 0.25, and 0.33, respectively. The others are actual urban sites in Central Tokyo (low-rise buildings area, street-canyon area, complex of high-rise and low-rise buildings area, and high-rise buildings area). The average building height, obstacle density, and building height variability of these four actual urban sites range from 9.6 to 34.1 m, from 0.39 to 0.56, and from 0.60 to 0.94, respectively.

Figure 3 shows the spatial distribution of building heights in actual urban areas used in LESs. In low-rise buildings area (Fig. 3a), most of the ground surface is covered with buildings with a height of about 10 m. In street-canyon area (Fig. 3b), street canyons are formed along main streets in densely built-up areas. In complex of high-rise and low-rise buildings area (Fig. 3c), high-rise buildings with a height greater than 100 m are sparsely arrayed. In high-rise buildings area (Fig. 3d), high-rise buildings with a height greater

than 100 m are densely arrayed. A plume is continuously released from the ground level in each urban area as shown in Fig. 3.

In order to investigate distribution patterns of plume concentrations influenced by urban surface geometries, we compare the spatial distributions of mean and r.m.s. concentrations in various urban areas with a wide range of obstacle density and building height variability.

3 Results

3.1 Approach flow

Figure 4 shows vertical profiles mean wind velocity and turbulence intensities of approach flow obtained by the LES. The thick and thin lines indicate the recommended data of **E**ngineering **S**cience **D**ata **U**nit 85020 (ESDU 85020, 1985) for moderate rough and rough surfaces, respectively. ESDU 85020 provides comprehensive turbulence characteristics of neutral atmospheric boundary layer. The vertical profile of the mean wind velocity of the LES is almost consistent with the profile of 0.25 power law. At the ground level, the LES data are a little underestimated. This difference is due to the influence of roughness blocks. Turbulence intensities for each component of the LES are found to be distributed between the vertical profiles of ESDU 85020 up to 300 m. The overestimation of the streamwise turbulence intensity is due to the rapid decrease of the mean wind velocity at the ground level.

Although there are a little differences in vertical profiles of the mean wind velocity and the streamwise turbulence intensity at the ground level, it is considered that our LES model reasonably produces a neutral boundary layer flow over rough surfaces.

3.2 Spatial distributions of mean and r.m.s. concentrations

Figure 5 shows the spatial distributions of mean concentration (C_{ave}) at the ground-level in actual urban areas. Mean concentrations are normalized by the initial concentration
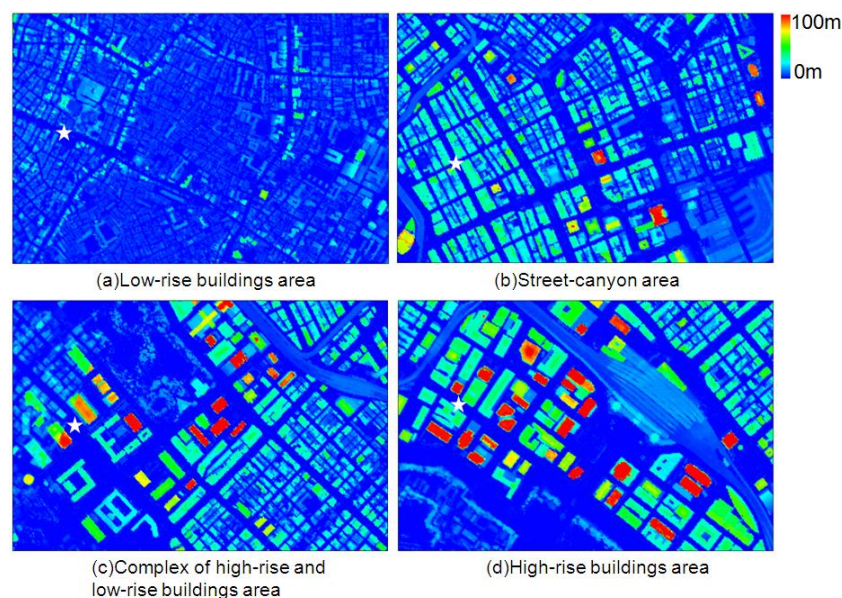
Figure 3. Spatial distributions of building heights in actual urban areas for LES calculation cases. The star depicts a ground-level plume source location.
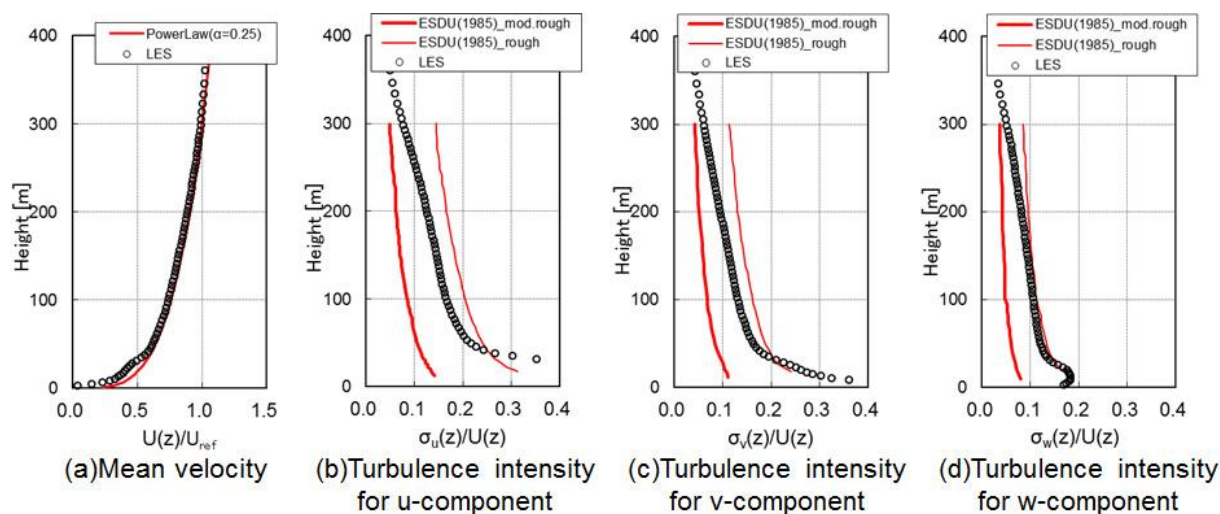

Figure 4. Turbulence characteristics of approach flow. The thik and thin lines indicate vertical profiles of ESDU 85020 for moderate rough and rough surfaces, respectively.

(C_{init}). In low-rise buildings area, the plume forms well-known Gaussian like pattern, where centerline of the plume follows the mean wind direction and a lateral spread steadily increases with the downwind distance. In street-canyon area, high mean concentration regions are formed along main streets near the point source and the plume centerlines shifted to the right due to the channeling effects of the wide street canyons. The initial lateral spread is larger than in the low-rise building area and gradually increase with a downwind distance. In complex of high-rise and low-rise buildings area, a plume is rapidly dispersed in the spanwise direction due to frequent cases of strong lateral winds caused by the sparsely

arrayed high-rise buildings near the point source. In high-rise buildings area, high mean concentration regions are formed around the point source due to the sheltering effects of densely arrayed high-rise buildings, while the spanwise plume spreads are greatly enhanced at the short distances.

Figure 6 shows the spatial distributions of normalized r.m.s. concentration ($C_{r.m.s.}$) by the initial concentration at the ground-level. In low-rise buildings area, r.m.s. concentrations gradually decrease with a downwind distance. In street-canyon area, high r.m.s. concentration regions are formed along the main streets. However, at a downwind distance from the point source greater than a few hundreds meter,
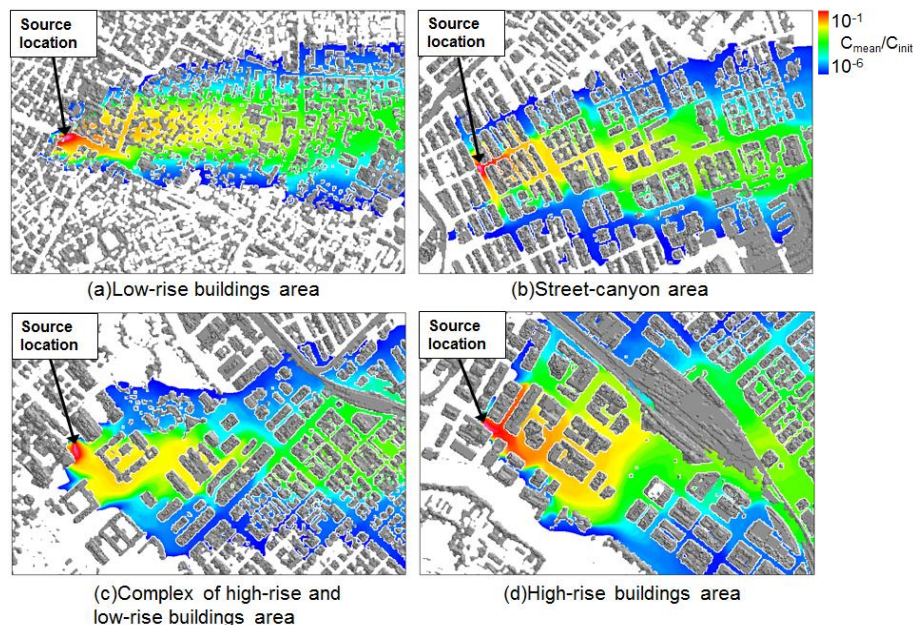
Figure 5. Spatial distributions of mean concentration at the ground-level in actual urban areas.
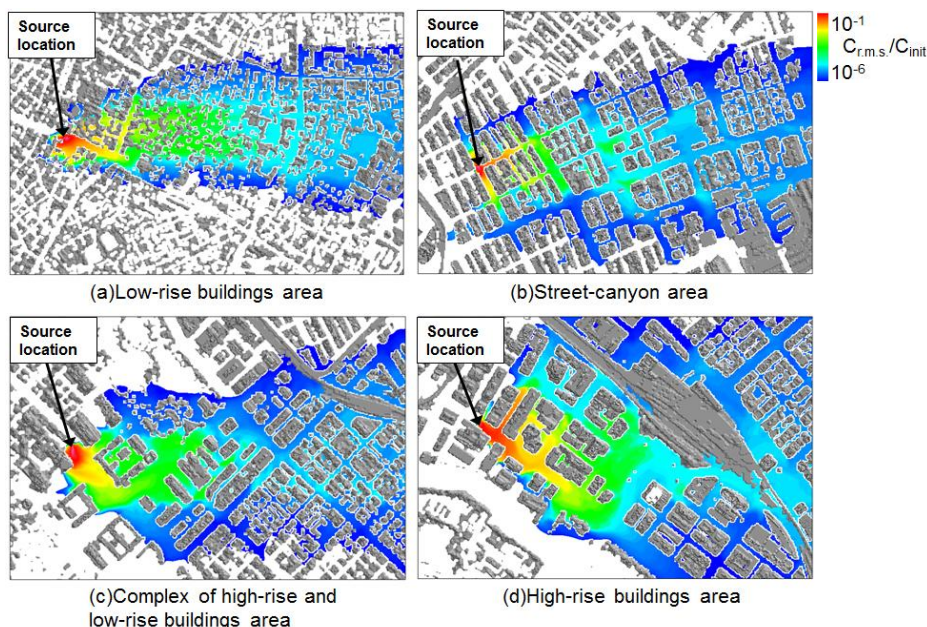

Figure 6. Spatial distributions of r.m.s. concentration at the ground-level in actual urban areas.

r.m.s. concentrations rapidly decrease. Also in complex of high-rise and low-rise buildings area, and high-rise buildings area, r.m.s. concentrations rapidly decrease with downwind distances while those are large around the point source. This is due to the smoothing effects of the small-scale turbulent eddies induced by the buildings on the concentration fluctuations.

3.3 Streamwise variation of mean and r.m.s. concentrations

Figures 7 and 8 compare streamwise variation of mean and r.m.s. concentrations at a height of 8.0 m with downwind distance from the point source. The experimental results (Bezpalcova and Ohba, 2008) show the concentration data within cubic buildings arrays. The LES results show those within cubic buildings arrays (Nakayama et al., 2013) and various
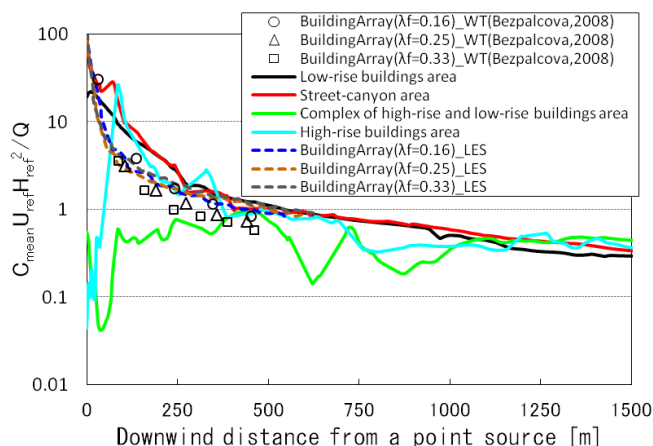
Figure 7. Streamwise variation of mean concentration at a height of 8.0 m from a point source.

Figure 8. Streamwise variation of r.m.s. concentration at a height of 8.0 m from a point source.

actual urban areas, respectively. They carried out wind tunnel experiments of plume dispersion in regularly square arrays of cubic buildings with obstacle density (λ_f) of 0.16, 0.25, and 0.33. In their experiments, the plume was released from the ground-level point source at the center just behind the building of the arrays in each case. U_{ref} is wind speed at 1.5 times building height $H_{ref} = 42$ m in the full scale condition when model scale was 1 : 400. Mean and r.m.s. concentrations are measured ones at a height of about 12 m. Q indicates source strength.

Mean concentrations (Fig. 7) in cubic building arrays of the experiment show different values depending on obstacle density for downwind distances shorter than a few hundreds meter and they converge at about 500 m from the point source. Those of the LES data also show the similar tendency to gradually decrease with a downwind distance among each case. In low-rise buildings area and street-canyon area, mean concentrations are found to gradually decrease with downwind distances. In complex of high-rise and low-rise buildings area and high-rise buildings area, there are quite scatters for downwind distances shorter than 1.0 km due to the particular position of the high-rise buildings. However, for downwind distances longer than 1.0 km from the point source, the mean concentrations are the same for all four urban settings.

For every cubic building array, the lateral mean concentration profiles are Gaussian-type curves at downstream positions. The layout of the building is very regular and the individual structures are relatively small compared to the real urban buildings. This set-up introduces significant mixing into the plume and the dependence on the building array density is weak. Therefore, the distribution patterns become similar among each case, which leads to convergence at a shorter distance than those in actual urban areas, where long wide boulevards may channel the flow and create heterogeneity.

R.m.s. concentrations (Fig. 8) in cubic building arrays of the experiment show small differences (mainly due to partic-
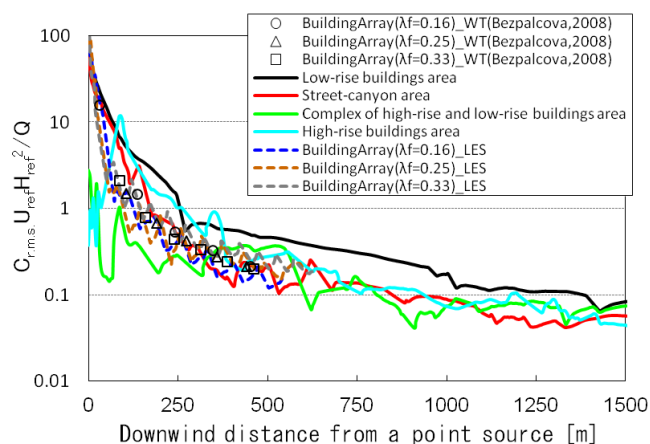
ular positions of individual buildings) near the point source and rapidly converge with the downwind distances. The LES data also show slight differences near the point source. However, the tendency to rapidly decrease with a downwind distance is almost the same among each cubic building array. In low-rise buildings area, a plume is deflected by the comparatively large-scale eddies which actively fluctuate the concentrations. Therefore, the decrease of r.m.s. concentrations for the downwind distance is small, comparing to in the other urban areas. In street-canyon area, r.m.s. concentrations values are comparable to those in the low-rise buildings area near the point source. However, those rapidly decrease with a downwind distance due to the smoothing effects of cavity flows in the street canyons. In complex of high-rise and low-rise buildings area and high-rise buildings area, r.m.s. scatter due to particular positions of individual buildings for downwind distances shorter than 1.0 km. This scatter is due to the local turbulent structures induced by the complex urban surface geometries. However, for downwind distances longer than 1.0 km from the point source, the differences of the r.m.s. concentration values among various urban areas are found to become small.

Macdonald and Griffiths (1997) carried out field experiments of plume dispersion through cubic building arrays with obstacle densities of 0.06, 0.16, and 0.44, and compared the variations of the lateral plume spreads and plume centerline concentrations with downwind distances from the point source. In their experimental results, it was shown that the influence of obstacle density on plume dispersion becomes small for downwind distances from the point source longer than 10 times building scale. In the full scale condition, this length corresponds to about 110 m. From their results and our LES results, it is considered that the influence of simple urban surface geometries on distribution patterns of plume concentrations becomes small for downwind distances longer than 500 m from the point source. Furthermore, from

our LES results for complex urban surface geometries, it is shown that the influence on those of plume concentrations becomes small for downwind distances longer than 1.0 km from the point source. These facts imply that the spatial extent of distribution patterns of a plume influenced by actual urban surface geometries is 1.0 km from the point source.

For the case of accidental or intentional release of toxic or flammable gases into the atmosphere, high concentration peaks need to be estimated. We carried out LESs of plume dispersion in cubic building arrays with obstacle densities of 0.16, 0.25, and 0.33, and evaluated the peak concentrations in comparison to the wind tunnel experimental data of Bezpalcova and Ohba (2008) (Nakayama et al., 2013). Although each building was resolved by 16 grid points in the lateral direction to accurately simulate turbulent behaviors (Santiago et al., 2008 and Xie and Castro, 2006), peak concentrations C_{99} defined as the value that is not exceeded by 99 % of the cumulative probability function of the concentration fluctuation were underestimated especially for denser arrays greater than obstacle density of 0.25. This indicates that it is unreasonable to directly estimate peak concentration values from the time series of the instantaneous concentrations. In such a situation, it is considered to be reasonable to apply theoretical models. There are typically three approaches, e.g. extreme value theory (Xie et al., 2004), probabilistic approaches (Csanady, 1973; Hanna, 1984), and deterministic approaches (Bartzis et al., 2007). The theoretical models can reasonably provide peak concentrations when statistic values of plume concentrations (mean concentrations, concentration variances, etc.) are obtained and will be practical for the safety analysis.

4 Conclusions

In this study, we compare the spatial distributions of mean and r.m.s. concentrations in various urban areas with a wide range of obstacle density and building height variability and investigate the spatial extent of distribution patterns of plume concentrations influenced by urban surface geometries by comparative analysis. Centerline mean concentration distributions for various complex urban surface geometries are converging for downwind distances from the point source greater than 1.0 km. The difference of r.m.s. concentration distributions among complex urban surface geometries also becomes small for downwind distances from the point source longer than 1.0 km. From these results, it can be concluded that a length of a computational model should be at least 1.0 km from a point source in order to capture distribution patterns of plume concentrations influenced by actual urban surface geometries.

The real form of accidental or intentional release in urban area is considered to be mainly instantaneous release. The continuous release has however many similar features. Although the exact relationship between concentration statis-

tics of continuously released plume and ensemble statistics of instantaneously released puffs is not known, we consider continuous release as a reasonable first estimate for an instantaneous release case. The reason to perform the continuous release case first is computational costs. It would require much longer model run to obtain representative ensemble of instantaneous releases. Our obtained results will be useful in local-scale dispersion modeling for emergency response.

References

Armand, P., Duchnne, C., Oldrini, O., Olry, C., and Moussafir, J.: Application of PMSS, the parallel version of MSS, to the micro-meteorological flow field and deleterious dispersion inside an extended simulation domain covering the whole Paris area, 14th International Conference on Harmonization within Atmospheric Dispersion Modelling for Regulatory Purpose, HARMO'14, 2–6 October, Kos, Greece, 2011.

Baklanov, A. A. and Nuterman, R. B.: Multi-scale atmospheric environment modelling for urban areas, Adv. Sci. Res., 3, 53–57, doi:10.5194/asr-3-53-2009, 2009.

Bartzis, J. G., Sfetsos, A., and Andronopoulos, S.: On the individual exposure from airborne hazardous releases: The effect of atmospheric turbulence, J. Hazard. Mater., 150, 76–82, 2007.

Bezpalcova, K. and Ohba, M.: Advective and turbulent vertical fluxes of the passive contaminant inside an urban canopy, Proceeding of 20th National Symposium on Wind Engineering, Tokyo, Japan, 20, 19–24, 2008.

Boris, J. P.: The threat of chemical and biological terrorism: preparing a response, Comput. Sci. Eng., 4, 22–32, 2002.

Csanady, G. T.: Turbulent Diffusion in the Environment, D. Reidel Publishing Co., Dordrecht, Holland, 222–248, 1973.

Engineering Science Data Unit: Characteristics of atmospheric turbulence near the ground Part 2 Single point data for strong winds (neutral atmosphere), ESDU Item, 85020, 1985.

Franke, J., Hellsten, A., Schlunzen, H., and Carissimo, B.: Best practice guideline for the CFD simulation of flows in the urban environment, COST Action 732, Quality assurance and improvement of microscale meteorological models, COST Office Brussels, ISBN: 3-00-018312-4, 2007.

Goldstein, D., Handler, R., and Sirovich, L.: Modeling a no-slip flow boundary with an external force field, J. Comput. Phys., 105, 354–366, 1993.

Gresho, P. M.: Some interesting issues in incompressible fluid dynamics, both in the continuum and in numerical simulation, Adv. Appl. Mech., 28, 45–140, 1992.

Hanna, S. R.: The exponential probability density function and concentration fluctuation in smoke plumes, Bound.-Lay. Meteorol., 29, 361–375, 1984.

Harlow, F. and Welch, J. E.: Numerical calculation of time-dependent viscous incompressible flow of fluid with a free surface, Phys. Fluids, 8, 2182–2189, 1965.

Kataoka, H. and Mizuno, M.: Numerical flow computation around aeroelastic 3D square cylinder using inflow turbulence, Wind Struct., 5, 379–392, 2002.

Macdonald, R. W. and Griffiths, R. F.: Field experiments of dispersion through regular arrays of cubic structures, 31, 783–795, Atmos. Environ., 1997.

Nakayama, H., Jurcakova, K., and Nagai, H.: Development of Local-Scale High-Resolution Atmospheric Dispersion Model Using Large-Eddy Simulation. Part 3: Turbulent Flow and Plume Dispersion in Building Arrays, Vol. 50, accepted, 2013.

Santiago, J. L., Coceal, O., Martilli, A., and Belcher, S. E.: Variation of the sectional drag coefficient of a group of buildings with packing density, Bound.-Lay. Meteorol., 128, 445–457, 2008.

Smagorinsky, J.: General circulation experiments with the primitive equations, Mon. Weather Rev., 91, 99–164, 1963.

Takewaki, H., Nishiguchi, A., and Yabe, T.: Cubic Interpolated Pseudo-particle method (CIP) for solving hyperbolic-type equations, J. Comput. Phys., 61, 261–268, 1985.

Tominaga, Y. and Stathopoulos, T.: Numerical simulation of dispersion around an isolated cubic building: Model evaluation of RANS and LES, Build. Environ., 45, 2231–2239, 2010.

Tominaga, Y. and Stathopoulos, T.: CFD modeling of pollution dispersion in a street canyon: Comparison between LES and RANS, J. Wind Eng. Ind. Aerodynamics, 99, 340–348, 2011.

Tominaga, Y., Mochida, A., Yoshie, R., Kataoka, H., Nozu, T., Yoshikawa, M., and Shirasawa, T.: AIJ guidelines for practical applications of CFD to pedestrian wind environment around buildings, J. Wind Eng. Ind. Aerodynamics, 96, 1749–1761, 2008.

Xie, Z. T. and Castro, I. P.: LES and RANS for turbulent flow over arrays of wall-mounted obstacles, Flow Turbul. Combust., 76, 291–312, 2006.

Xie, Z. T., Hayden, P., Voke, P. R., and Robins, A. G.: Large-eddy simulation of dispersion: comparison between elevated source and ground level source, J. Turbul., 5, 1–16, 2004.